

SHEP 95/30
hep-ph/9601230
January 1996

Chargino Production at LEP2 in a Supergravity Model

Marco A. Díaz and Steve F. King

*Physics Department, University of Southampton
Southampton, SO17 1BJ, U.K.*

Abstract

In the framework of a particular supergravity model which provides a natural solution to the μ -problem we show how the discovery of a chargino at LEP2 and the measurement of its mass and production cross-section, together with the measurement of the mass of the lightest neutralino, would determine the entire Higgs and SUSY spectrum. We give detailed predictions for the Higgs and SUSY spectrum as a function of the chargino production cross-section, for constant values of the lightest chargino and gluino masses.

Recently LEP1.5 has set a new lower bound on the lightest chargino mass of about 65 GeV if $m_{\tilde{\chi}_1^\pm} - m_{\tilde{\chi}_1^0} \gtrsim 10$ GeV [1]. In general LEP2 will be able to bound or discover charginos up to the kinematic limit of the machine. In this paper we explore the possible consequences of chargino discovery at LEP2 within the framework of a well motivated supergravity model.

It is well known that, with the assumption of a universal gaugino mass $M_{1/2}$, the chargino $\tilde{\chi}_i^\pm$ ($i = 1, 2$) and neutralino $\tilde{\chi}_i^0$ ($i = 1 \dots 4$) masses and mixing angles only depend on three unknown parameters: the gluino mass $m_{\tilde{g}}$, μ and $\tan \beta$ [2]. In a recent paper [3] we have shown how the discovery of the lightest chargino at LEP2 and the measurement of its mass, $m_{\tilde{\chi}_1^\pm}$, and production cross-section, $\sigma(e^+e^- \rightarrow \tilde{\chi}_1^+ \tilde{\chi}_1^-)$, together with the measurement of the mass of the lightest neutralino, $m_{\tilde{\chi}_1^0}$, will enable the basic parameters $m_{\tilde{g}}$, μ and $\tan \beta$ to be determined, up to certain ambiguities (see also ref. [4]).

In the present paper we shall extend the above analysis from the gaugino sector of the Minimal Supersymmetric Standard Model (MSSM) [5] to the entire supersymmetric (SUSY) and Higgs spectrum. However, whereas the gaugino sector is completely specified by three parameters, the remaining spectrum depends on very many parameters and without some simplifying principle it is impossible to make progress. Therefore in the present paper we shall explore the consequences of a specific supergravity (SUGRA) model which has sufficient predictive power to enable the entire Higgs and SUSY spectrum to be deduced from just the LEP2 measurements $m_{\tilde{\chi}_1^\pm}$, $\sigma(e^+e^- \rightarrow \tilde{\chi}_1^+ \tilde{\chi}_1^-)$, and $m_{\tilde{\chi}_1^0}$ – a result which underlines both the importance of LEP2 and the power of supergravity.

The phenomenologically simplest SUGRA models typically involve universal soft parameters (at the unification scale ¹): m_0 , $M_{1/2}$, A , B in the usual notation corresponding to the universal scalar mass, gaugino mass, trilinear dimensionful coupling and $B\mu H_1 H_2$ term, respectively. Thus the squark and slepton soft masses are proportional to unit matrices in flavor space, and trilinear couplings are proportional to Yukawa matrices at the unification scale. Specific SUGRA models may involve further relationships between the soft parameters, for example the so-called minimal SUGRA model predicts that $B = A - m_0$ [6]. However this model involves an unnaturally small dimensional μ parameter appearing in the superpotential – the μ problem. Recently there have been several alternative mechanisms proposed to solve

¹We shall take apply these boundary conditions at the gauge coupling unification scale M_X , neglecting any effects due to running between the Planck scale and M_X .

the μ problem [7] and it is a common tendency of such models to predict $B = 2m_0$, although it is not clear why such different theories should lead to the same boundary condition. Therefore in the present paper we shall focus on SUGRA models which predict $B = 2m_0$ which have a stronger theoretical motivation.

According to the above discussion, the 5 independent parameters at M_X are: $B = 2m_0$, $M_{1/2}$, A , μ , h_{t0} , where h_{t0} is the top quark Yukawa coupling at M_X . We shall require radiative electroweak symmetry breaking, and impose the usual Higgs minimisation conditions at low energy. We consider all the supersymmetric mass parameters to be smaller than $M_{SUSY} = 1$ TeV. The order of magnitude of this scale emerges naturally when the model is embedded into a GUT [8]. In addition, to break radiatively the electroweak symmetry without fine-tuning the initial parameters M_{SUSY} cannot be too large [9]. Our 4 input parameters are chosen to be: m_t , $m_{\tilde{\chi}_1^\pm}$, μ and $m_{\tilde{g}}$ which are sufficient to specify the 5 independent parameters at M_X , given the requirement of correct electroweak symmetry breaking. The idea behind this choice of input parameters is that the top quark mass is measured at the Tevatron, and the chargino mass may be measured at LEP2. This only leaves the parameters μ and $m_{\tilde{g}}$ which can in principle be determined at LEP2 from a measurement of $\sigma(e^+e^- \rightarrow \tilde{\chi}_1^+ \tilde{\chi}_1^-)$ and $m_{\tilde{\chi}_1^0}$, as discussed in our previous analysis [3] except that now the electron sneutrino contribution to the cross-section will be taken into account. The main difference is of course that now these LEP2 measurements will serve to determine the *entire* Higgs and SUSY spectrum, not just the gaugino sector.

Our detailed procedure is to first fix values of top quark mass, chargino mass and gluino mass. For a given choice of μ , knowledge of $m_{\tilde{\chi}_1^\pm}$ and $m_{\tilde{g}}$ enables a determination of $\tan\beta$. With m_t and $\tan\beta$ specified we have a determination of h_t (at low energy) and hence h_{t0} (at high energy). With h_{t0} known, we choose values of m_0 and A and run all the parameters down to low energy (the RG equations do not depend on B). We do not take into account threshold corrections. The tree-level minimisation condition on the Higgs masses at low energy ²

$$(m_1^2 + \mu^2 + \frac{1}{2}M_Z^2 \cos 2\beta)(1 + \cos 2\beta) = (m_2^2 + \mu^2 - \frac{1}{2}M_Z^2 \cos 2\beta)(1 - \cos 2\beta) \quad (1)$$

where m_1^2 and m_2^2 are the soft SUSY breaking Higgs masses, will not in general be satisfied, and so we vary m_0 until it is. Sometimes there will be no solution for any value of $m_0^2 > 0$, and this condition has a big effect in reducing the allowed parameter space. Eq. (1) describes the minimization of the Higgs potential when the one-loop

²Each of these terms is equal to $\frac{1}{2}m_A^2(1 - \cos^2 2\beta)$, where m_A is the CP-odd scalar mass.

contributions to the effective potential are neglected. Having consistently determined m_0 we then find the low energy value of B using $B\mu = \frac{1}{2}m_A^2 \sin 2\beta$, and run it up to find the high energy value of B . In general the condition $B = 2m_0$ will not be satisfied, and we iterate the procedure for different values of A until this condition is met, which effectively serves to determine A . If we have chosen a suitable value of μ we will then have a successful data point from which the entire Higgs and SUSY spectrum may be calculated, and $\sigma(e^+e^- \rightarrow \tilde{\chi}_1^+ \tilde{\chi}_1^-)$ computed. We note that there is no ambiguity in the sign of the supersymmetric Higgs mass parameter μ , as opposed to global supersymmetry analyzed in ref. [3], because the high energy relation $B = 2m_0$ together with the low energy constraint $m_A^2 = 2B\mu/\sin(2\beta) > 0$ implies that only $\mu > 0$ solutions are satisfactory [7] (see also [10]).

Using the above procedure, contours in the $\sigma(e^+e^- \rightarrow \tilde{\chi}_1^+ \tilde{\chi}_1^-) - m_{\tilde{\chi}_1^0}$ plane for a fixed values of m_t , $m_{\tilde{\chi}_1^\pm}$ and $m_{\tilde{g}}$ are produced by varying μ over its successful range. These contours are shown in Figure 1. We see four groups of curves corresponding to the choices $m_{\tilde{\chi}_1^\pm} = 60, 70, 80$, and 90 GeV. We have taken $m_t = 176$ GeV and $\alpha_s = 0.116$. We do not find acceptable solutions for $m_{\tilde{\chi}_1^\pm} = 50$, consistent with the LEP1 experimental lower bound on the chargino mass $m_{\tilde{\chi}_1^\pm} > 45$ GeV [11, 12, 13]. For each value of the chargino mass, the different curves are labeled by the value of the gluino mass. It is clear from the figure that heavier charginos produce smaller total cross sections and, at the same time, they are associated with heavier neutralino 1, $\tilde{\chi}_1^0$. This neutralino is the lightest supersymmetric particle, or LSP. Since the LSP should be neutral, some curves for the case $m_{\tilde{\chi}_1^\pm} = 90$ GeV are truncated at high values of $\tan\beta$ because beyond that point the $\tilde{\tau}_1^\pm$ becomes lighter than $\tilde{\chi}_1^0$. It can also be appreciated from Fig. 1 that larger $m_{\tilde{g}}$ produce, in general, smaller cross sections. The reason here is that the sneutrino becomes lighter at larger gluino masses, and since the sneutrino contribution to the total cross section is negative, the total cross section decreases. Note that contours in Fig. 1 are truncated at the upper end (large cross-section end) where $\tan\beta$ is small, and at the lower end (small cross-section end) where $\tan\beta$ is large, for reasons which will become apparent. Fig. 1 clearly demonstrates that for a given m_t , LEP2 measurements of $m_{\tilde{\chi}_1^\pm}$, $\sigma(e^+e^- \rightarrow \tilde{\chi}_1^+ \tilde{\chi}_1^-)$ and $m_{\tilde{\chi}_1^0}$ are sufficient to completely specify all the parameters in the theory.

To emphasise that all the basic parameters of the theory, and with them, the whole Higgs and SUSY spectrum, are determined for each point of each contour in Fig. 1, we shall present a series of contours with $\sigma(e^+e^- \rightarrow \tilde{\chi}_1^+ \tilde{\chi}_1^-)$ along the vertical axis and some other determined quantity along the horizontal axis. In Figure 2

we show the set of $m_{\tilde{\chi}_1^\pm}$, $m_{\tilde{g}}$ contours corresponding to Fig. 1 but with the basic parameters (a) m_0 , (b) A , (c) $\tan\beta$ and (d) μ along the horizontal axes. For a given chargino mass, the gluino masses we have taken are bounded from above because gluinos heavier than some value produce solutions with $m_0^2 < 0$ [Fig. 2(a)], and from below because gluinos lighter than some value need values of A larger than 1 TeV [Fig. 2(b)]. We do not consider constraints from charge and color breaking [14]. The parameter $\tan\beta$ is plotted in Fig. 2(c), and the most noticeable feature is that many curves are truncated at $\tan\beta \approx 2$. The reason is that we are close to the fixed point of the top quark Yukawa coupling, and smaller values of $\tan\beta$ makes this coupling diverge at scales smaller than the unification scale. In the case of the lightest gluino choice, the fixed point of h_t is not reached, and the curve is truncated at higher values of $\tan\beta$ because the parameter A becomes larger than 1 TeV. For a fixed value of $m_{\tilde{\chi}_1^\pm}$ and $m_{\tilde{g}}$, the parameter μ is determined by the value of $\tan\beta$ and it is plotted in Fig. 2(d). Typically, the smaller the chargino mass is, the smaller the parameter μ is. Nevertheless, it never reaches values smaller than 150 GeV.

In Figure 3 we show the contours corresponding to Figure 1 but with (a) the second lightest neutralino mass, (b) the sneutrino mass, (c) the lightest charged slepton mass and (d) the lightest up-type squark mass along the horizontal axis. In Fig. 3(a) we see the production cross section as a function of $m_{\chi_2^0}$. This mass is strongly correlated with the lightest chargino mass, satisfies $m_{\chi_2^0} \gtrsim m_{\tilde{\chi}_1^\pm}$, and receives small increases as we increase the gluino mass. Similarly to the lightest neutralino case, the groups of curves corresponding to different values of $m_{\tilde{\chi}_1^\pm}$ are well differentiated, implying that we will have a very good idea of the mass of this particle even if we have large experimental errors on the LEP measurements mentioned before. The sneutrino mass is presented in Fig. 3(b). Note that it is the electron sneutrino that is of interest to us because it contributes to the chargino production cross section. Nevertheless, the three sneutrino flavors are practically degenerated in mass. The sneutrino mass always satisfies the experimental constraint $m_{\tilde{\nu}} > 41.8$ GeV [11, 15] and is represented in the figure by a vertical dotted line. It can be appreciated that the sneutrino contribution to the total chargino production cross section is more important when charginos are light, and that it decouples as $m_{\tilde{\nu}}$ increases. In Fig. 3(c) we plot the lightest charged slepton mass, which in all cases is $\tilde{\tau}_1^\pm$. The experimental LEP1 constraint $m_{\tilde{\tau}_1^\pm} > 45$ GeV [11, 12, 16] restricts the allowed parameter space, and consequently some of the curves (the ones with lighter gluino) are truncated at large $\tan\beta$. The reason for that lies in the left-right mixing of the mass matrix, because it is proportional to $m_\tau \mu \tan\beta$, and large values of $\tan\beta$ produce a large mass splitting between τ_1^\pm and

τ_2^\pm . The lightest of the up-type squarks is plotted in Fig. 3(d), which is predominantly the lightest stop, \tilde{t}_1 , with a small component of scharm (in all cases smaller than a percent). At small values of the universal scalar mass parameter m_0 , where the total cross section is small, the mass of the lightest up-type squark increases with this parameter m_0 . Nevertheless, for large values of m_0 the trilinear mass parameter A also is large, producing a large top squark mass mixing and consequently, a lighter \tilde{t}_1 . This makes the curves in Fig. 3(d) to turn towards the small values of the lightest up-type squark as the total cross section increases. Lighter \tilde{t}_1 are obtained when small chargino masses are considered, a combination that produces large corrections to the $Z \rightarrow b\bar{b}$ decay. Nevertheless, we do not find top squarks lighter than about 180 GeV, claimed to be necessary to explain the discrepancy between theory and experiment (see for example [17]).

The Higgs sector of the MSSM [18] is completely specified at tree level by the CP-odd Higgs mass m_A and $\tan\beta$. Nevertheless, a strong dependence on m_t and $m_{\tilde{t}}$ is introduced through radiative corrections to the charged Higgs mass [19, 20] and to the lightest neutral CP-even Higgs mass [20, 21]. In Figure 4 we show the corresponding contours of Fig. 1 with (a) the lightest CP-even Higgs boson mass, (b) the CP-odd Higgs boson mass, (c) the charged Higgs boson mass and (d) the value of $\cos(\beta - \alpha)$ along the horizontal axes. In this scenario, the lightest Higgs mass plotted in Fig. 4(a) is always smaller than 103 GeV, with obvious relevance for LEP2 [22]. The higher values of m_h are obtained when $\tan\beta$ is large, where the tree level contribution to m_h is maximum. On the other hand, at $\tan\beta \sim 2$ the lightest Higgs mass is minimum, with a lower bound of about 80 GeV. In the calculation of m_h we include the exact one-loop radiative corrections from top and bottom quarks and squarks and leading logarithms from the rest of the particles, working in an on-shell scheme where the parameter $\tan\beta$ is defined through the $A\tau^+\tau^-$ coupling [23]. We also include the dominant two-loop QCD corrections [24] and we sum all the leading and next-to-leading logarithms with a RGE technique. The mass of the CP-odd Higgs m_A is plotted in Fig. 4(b). It is obtained from eq. (1) which comes from the minimization of the Higgs potential. This particle is in all cases heavier than about 130 GeV, what makes it difficult to be observed at LEP2. The charged Higgs mass, plotted in Fig. 4(c), is strongly correlated to the value of m_A , because at tree level the relation $m_{H^\pm}^2 = m_W^2 + m_A^2$ holds. We include the one-loop radiative correction to this mass, nevertheless, in the region of parameter space considered here, the correction is smaller than ~ 2 GeV in all cases. Finally, in Fig. 4(d) we plot the parameter $-\cos(\beta - \alpha)$ which controls the ZZH coupling. One-loop corrections to

this angle are already taken into account [25]. The fact that this parameter remains small implies that the heavy Higgs boson H is weakly coupled to the Z -boson. At the same time the lightest Higgs h , with a ZZh coupling proportional to $\sin(\beta - \alpha)$, has couplings that approach the corresponding Standard Model (SM) Higgs boson couplings. Nevertheless, it is worth mentioning that, if we consider the SM with no new physics below $\sim 10^{10}$ GeV and the MSSM with $M_{SUSY} \lesssim 1$ TeV, the allowed values of $m_{H_{SM}}$ are always greater than m_h providing the top quark is sufficiently heavy [26].

Finally we return to our original question: what can we learn from this SUGRA model with the detection of charginos at LEP2? The answer is summarised in Fig. 1. In this figure a group of curves corresponding to a particular value of $m_{\tilde{\chi}_1^\pm}$ are well differentiated from a group corresponding to a different value. This permits us to check the validity of the model even if the experimental errors are so large that it is not possible to precisely differentiate the curves labeled by the value of the gluino mass. Assuming that precise measurements of the total cross section $\sigma(e^+e^- \rightarrow \tilde{\chi}_1^+ \tilde{\chi}_1^-)$, the chargino mass $m_{\tilde{\chi}_1^\pm}$, and the lightest neutralino mass are available, it is possible to predict the value of $m_{\tilde{g}}$, and from Figs. 2–4 the rest of the parameters of the model and the masses of the physical particles can be predicted within this particular well motivated SUGRA model. For example a firm prediction of this model is that if LEP2 discovers a chargino then the lightest CP-even Higgs boson must be lighter than 103 GeV and have SM-like couplings.

Acknowledgements

One of us (MAD) has benefited from discussions with B. de Carlos on different aspects of this problem and is thankful to A. Casas for clarifying the origin of the relation $B = 2m_0$.

References

- [1] L. Rolandi, H. Dijkstra, D. Strickland and G. Wilson, representing the ALEPH, DELPHI, L3 and OPAL Collaborations, Joint Seminar on the First Results from LEP1.5, CERN, Dec. 12th, 1995.
- [2] J.F. Gunion and H.E. Haber, *Nucl. Phys.* **B272**, 1 (1986).
- [3] M.A. Díaz and S.F. King *Phys. Lett. B* **349**, 105 (1995).
- [4] J. Feng and M. Strassler, *Phys. Rev. D* **51**, 4661 (1995).
- [5] H.P. Nilles, *Phys. Rep.* **110**, 1 (1984); H.E. Haber and G.L. Kane, *Phys. Rep.* **117**, 75 (1985); R. Barbieri, *Riv. Nuovo Cimento* **11**, 1 (1988).
- [6] R. Barbieri, S. Ferrara and C. A. Savoy, *Phys. Lett. B* **119**, 343 (1982).
- [7] G.F. Giudice and A. Masiero, *Phys. Lett. B* **115**, 480 (1988); J.A. Casas and C. Muñoz, *Phys. Lett. B* **306**, 288 (1993); G.F. Giudice and E. Roulet, *Phys. Lett. B* **315**, 107 (1993); A. Brignole, L.E. Ibañez and C. Muñoz, *Nucl. Phys. B* **422**, 125 (1994).
- [8] P. Langacker and M. Luo, *Phys. Rev. D* **44**, 817 (1991); U. Amaldi, W. de Boer, and H. Furstenau, *Phys. Lett. B* **260**, 447 (1991); J. Lopez, D. V. Nanopoulos, H. Pois, X. Wang, and A. Zichichi, *Phys. Lett. B* **306**, 73 (1993); G. L. Kane, C. Kolda, L. Roszkowski, and J. D. Wells, *Phys. Rev. D* **49**, 6173 (1994).
- [9] B. de Carlos and J.A. Casas, *Phys. Lett. B* **309**, 320 (1993).
- [10] B. de Carlos and J.A. Casas, *Phys. Lett. B* **349**, 300 (1995); erratum-ibid. *B* **351** 604 (1995).
- [11] L3 Collaboration (O. Adriani et al.), *Phys. Rep.* **236**, 1 (1993); The ALEPH Collaboration (D. Decamp et al.), *Phys. Rep.* **216**, 253 (1992).
- [12] DELPHI Collaboration (Abreu et al.), *Phys. Lett. B* **247**, 157 (1990); OPAL Collaboration (Akrawy et al.), *Phys. Lett. B* **240**, 261 (1990).
- [13] TOPAZ Collaboration (Adachi et al.), *Phys. Lett. B* **244**, 352 (1990); UA2 Collaboration (Akesson et al.), *Phys. Lett. B* **238**, 442 (1990); Mark II Collaboration (Barklow et al.), *Phys. Rev. Lett.* **64**, 2984 (1990).

- [14] J.A. Casas, Santa Cruz Report No. SCIPP-95-48, Nov. 1995, and references therein.
- [15] DELPHI Collaboration (Abreu et al.), *Nucl. Phys. B* **367**, 511 (1991); OPAL Collaboration (Alexander et al.), *Z. Phys. C* **52**, 175 (1991).
- [16] AMY Collaboration (Sakai et al.), *Phys. Lett. B* **234**, 534 (1990); VENUS Collaboration (Taketani et al.), *Phys. Lett. B* **234**, 202 (1990); TOPAZ Collaboration (Adachi et al.), *Phys. Lett. B* **218**, 105 (1989); UA1 Collaboration (Albajar et al.), *Z. Phys. C* **44**, 15 (1989).
- [17] J.D. Wells, C. Kolda and G.L. Kane, *Phys. Lett. B* **338**, 219 (1994).
- [18] J.F. Gunion, H.E. Haber, G. Kane and S. Dawson, *The Higgs Hunter's Guide* (Addison-Weslwy, Redwood City, CA, 1990).
- [19] J.F. Gunion and A. Turski, *Phys. Rev. D* **39**, 2701 (1989); **40**, 2333 (1989); A. Brignole, J. Ellis, G. Ridolfi, and F. Zwirner, *Phys. Lett. B* **271**, 123 (1991); M.A. Díaz and H.E. Haber, *Phys. Rev. D* **45**, 4246 (1992); A. Brignole, *Phys. Lett. B* **277**, 313 (1992).
- [20] M.S. Berger, *Phys. Rev. D* **41**, 225 (1990); P.H. Chankowski, S. Pokorski, and J. Rosiek, *Phys. Lett. B* **274**, 191 (1992); K. Sasaki, M. Carena, and C.E.M. Wagner, *Nucl. Phys. B* **381**, 66 (1992); M. Drees and M.M. Nojiri, *Phys. Rev. D* **45**, 2482 (1992); H.E. Haber and R. Hempfling, *Phys. Rev. D* **48**, 4280 (1993).
- [21] H.E. Haber and R. Hempfling, *Phys. Rev. Lett.* **66**, 1815 (1991); A. Yamada, *Phys. Lett. B* **263**, 233 (1991); Y. Okada, M. Yamaguchi and T. Yanagida, *Phys. Lett. B* **262**, 54 (1991); Y. Okada, M. Yamaguchi and T. Yanagida, *Prog. Theor. Phys.* **85**, 1 (1991); J. Ellis, G. Ridolfi and F. Zwirner, *Phys. Lett. B* **257**, 83 (1991); R. Barbieri, M. Frigeni, F. Caravaglios, *Phys. Lett. B* **258**, 167 (1991); J. Ellis, G. Ridolfi and F. Zwirner, *Phys. Lett. B* **262**, 477 (1991); J.L. Lopez and D.V. Nanopoulos, *Phys. Lett. B* **266**, 397 (1991); A. Brignole, *Phys. Lett. B* **281**, 284 (1992); D.M. Pierce, A. Papadopoulos, and S. Johnson, *Phys. Rev. Lett.* **68**, 3678 (1992); M.A. Díaz and H.E. Haber, *Phys. Rev. D* **46**, 3086 (1992); A. Yamada, *Z. Phys. C* **61**, 247 (1994); P.H. Chankowski, S. Pokorski, and J. Rosiek, *Nucl. Phys. B* **423**, 437 (1994); A. Dabelstein, *Z. Phys. C* **67**, 495 (1995).
- [22] J. F. Gunion, "Searching for the Higgs Boson(s)", to appear in Proc. of the Zeuthen Workshop — LEP200 and Beyond, Teupitz/Brandenburg, Germany,

- 10–15 April, 1994, eds. T Riemann and J Blumlein; A. Djouadi, J. Kalinowski and P. M. Zerwas, *Z. Phys.* **C57**, 569 (1993); V. Barger, K. Cheung, A. Djouadi, B. A. Kniehl, and P. M. Zerwas, *Phys. Rev. D* **49**, 79 (1994); A. Djouadi, *Int. J. Mod. Phys.* **A10**, 1 (1995).
- [23] M.A. Díaz, *Phys. Rev. D* **48**, 2152 (1993).
- [24] R. Hempfling and A.H. Hoang, *Phys. Lett. B* **331**, 99 (1994).
- [25] M.A. Díaz, preprint VAND–TH–94–19 (hep-ph-9408320), presented at 1994 Meeting of the APS, DPF’94, Albuquerque, New Mexico, 2-6 Aug. 1994.
- [26] N.V. Krasnikov and S. Pokorski, *Phys. Lett. B* **288**, 184 (1992); M.A. Díaz, T.A. ter Veldhuis, and T.J. Weiler, *Phys. Rev. Lett.* **74**, 2876 (1995); J.A. Casas, J.R. Espinosa, and M. Quirós, *Phys. Lett. B* **342**, 171 (1995); M.A. Díaz, T.A. ter Veldhuis, and T.J. Weiler, Preprint No. VAND-TH-94-14-UPD and SHEP-95-08 (hep-ph-9512229), Dec. 1995.

Figure Captions:

Fig. 1. Total cross section of chargino pair production from e^+e^- annihilation as a function of the mass of the lightest neutralino for constant values of the lightest chargino and the gluino masses. Four groups of curves are shown corresponding to $m_{\tilde{\chi}_1^\pm} = 60$ GeV (dotdash), 70 GeV (solid), 80 GeV (dashes), and 90 GeV (dots), with each line labelled by the gluino mass in GeV.

Fig. 2. Total chargino pair production cross section as a function of four different parameters that characterize the supergravity model. (a) The universal scalar mass m_0 , (b) the universal trilinear coupling A , (c) the ratio of the two Higgs vacuum expectation values $\tan\beta$, and (d) the Higgs mass parameter μ . There is a one-to-one correspondence between the lines in this Figure and those in Figure 1. The line styles for the chargino masses are as in Figure 1. For each chargino mass the gluino masses also correspond to those in Figure 1. Although we have not labelled the gluino mass, it should be possible to distinguish which line corresponds to which gluino mass by comparing the total cross-section for chargino production plotted here to that plotted in Figure 1.

Fig. 3. Total chargino pair production cross section as a function of the mass of (a) the second lightest neutralino, (b) the sneutrino, (c) the lightest charged slepton, and (d) the lightest up-type squark. There is a one-to-one correspondence between the lines in this Figure and those in Figure 1. The line styles for the chargino masses are as in Figure 1. For each chargino mass the gluino masses also correspond to those in Figure 1. Although we have not labelled the gluino mass, it should be possible to distinguish which line corresponds to which gluino mass by comparing the total cross-section for chargino production plotted here to that plotted in Figure 1.

Fig. 4. Total chargino pair production cross section as a function of four different parameters in the Higgs sector. (a) The lightest Higgs mass, (b) the CP-odd Higgs mass, (c) the charged Higgs mass, and (d) the parameter $-\cos(\beta - \alpha)$ whose magnitude is the coupling of the heavy CP-even Higgs to a pair of Z -bosons. There is a one-to-one correspondence between the lines in this Figure and those in Figure 1. The line styles for the chargino masses are as in Figure 1. For each chargino mass the gluino masses also correspond to those in Figure 1. Although we have not labelled the gluino mass, it should be possible to distinguish which line corresponds to which gluino mass by comparing the total cross-section for chargino production plotted here to that plotted in Figure 1.

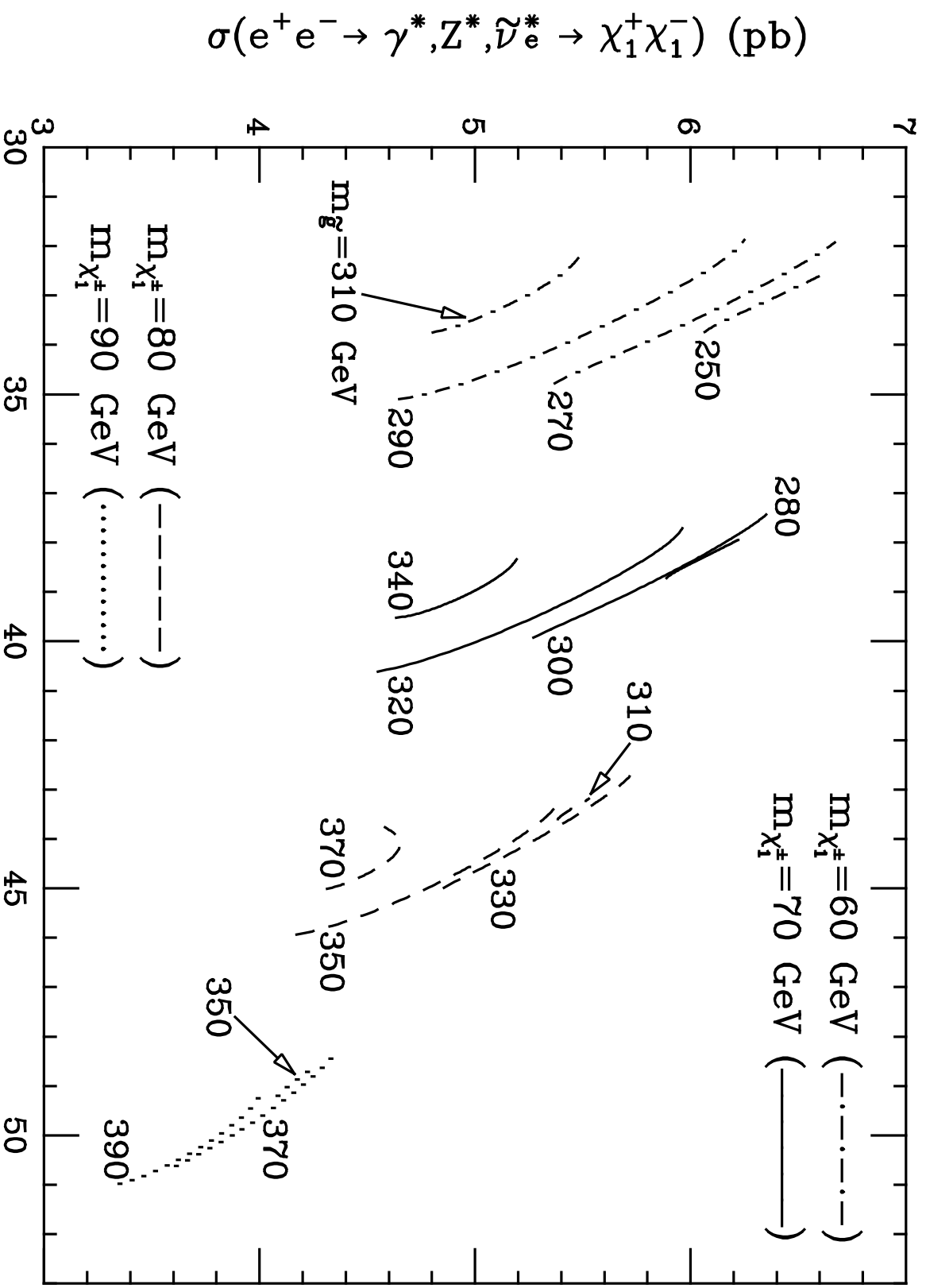


Fig. 1

$$\sigma(e^+e^- \rightarrow \gamma^*, Z^*, \tilde{\nu}_e^* \rightarrow \chi_1^+ \chi_1^-) \text{ (pb)}$$

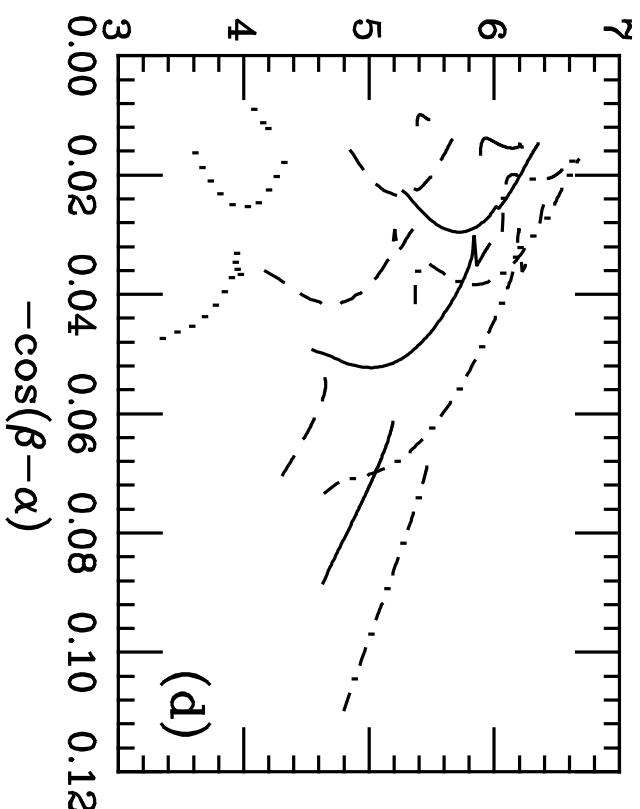
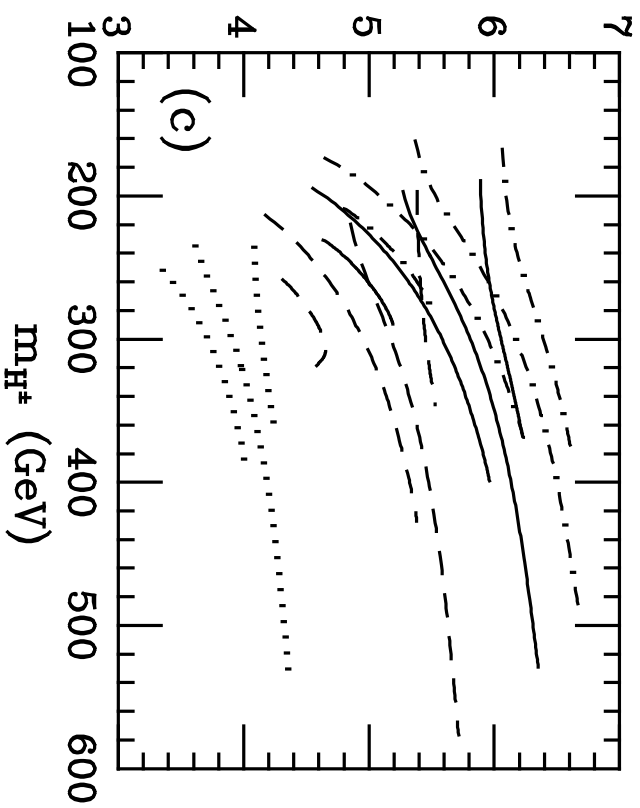
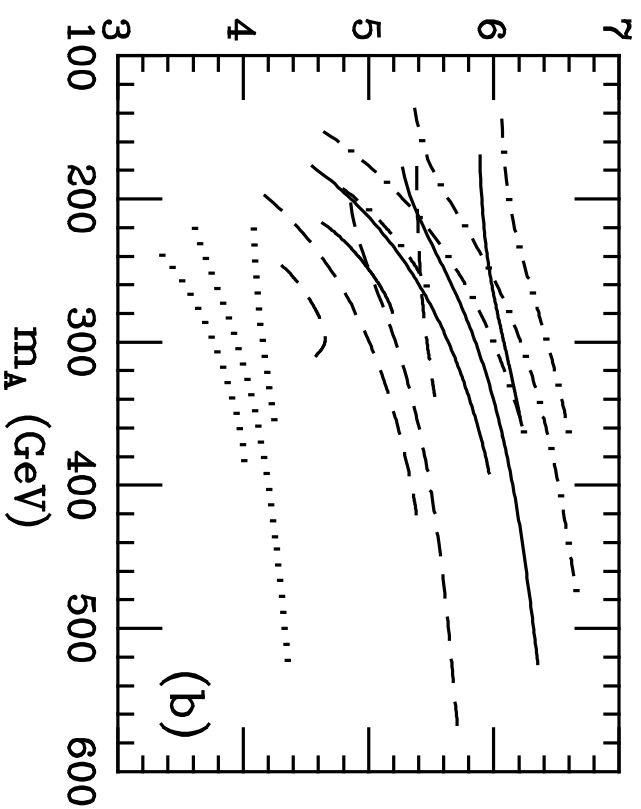
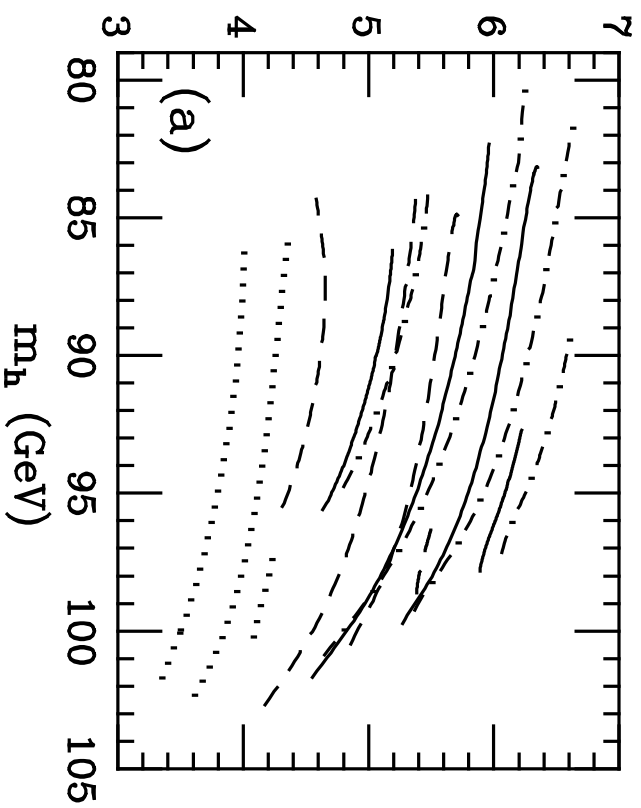


Fig. 4

$$\sigma(e^+e^- \rightarrow \gamma^*, Z^*, \tilde{\nu}_e^* \rightarrow \chi_1^+ \chi_1^-) \text{ (pb)}$$

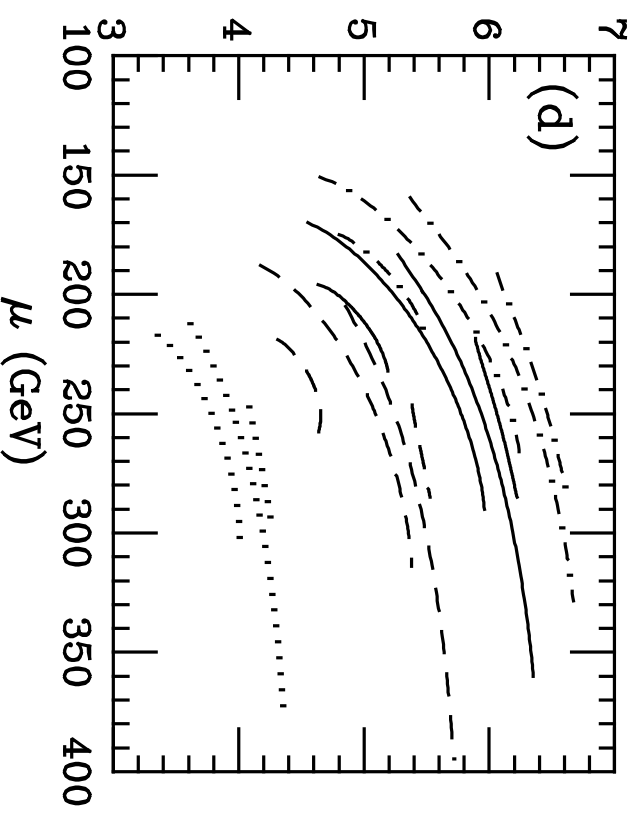
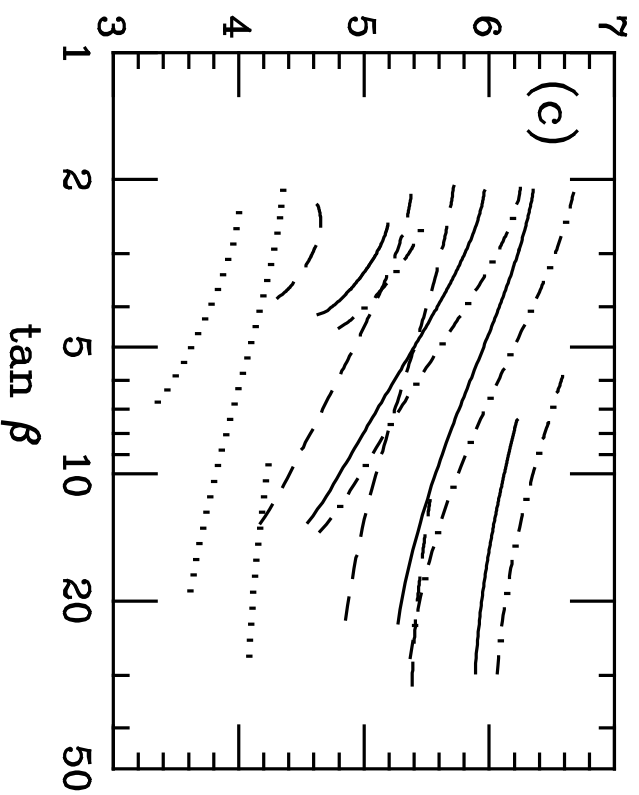
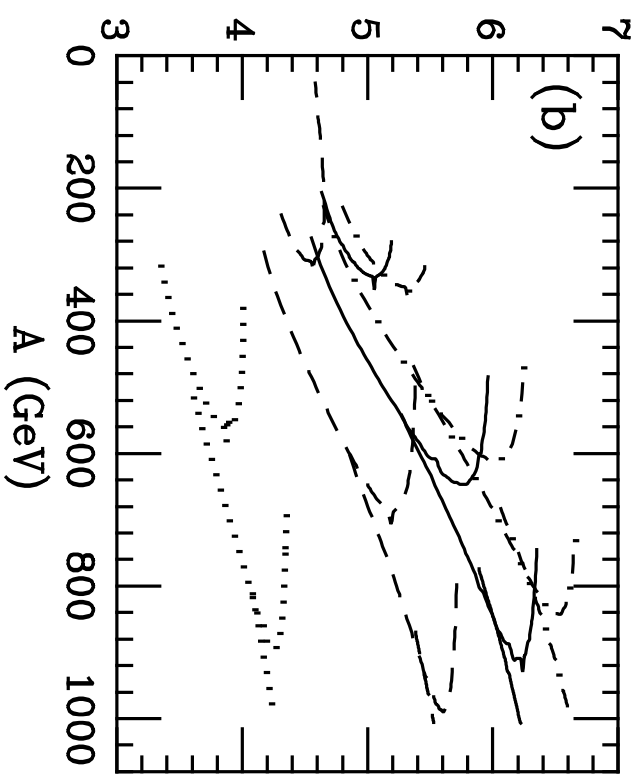
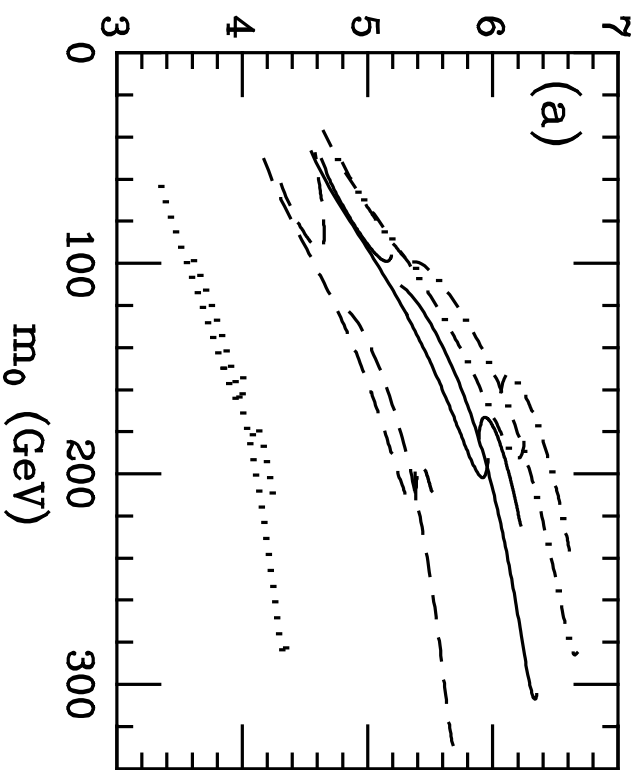


Fig. 2

$$\sigma(e^+e^- \rightarrow \gamma^*, Z^*, \tilde{\nu}_e^* \rightarrow \chi_1^+ \chi_1^-) \text{ (pb)}$$

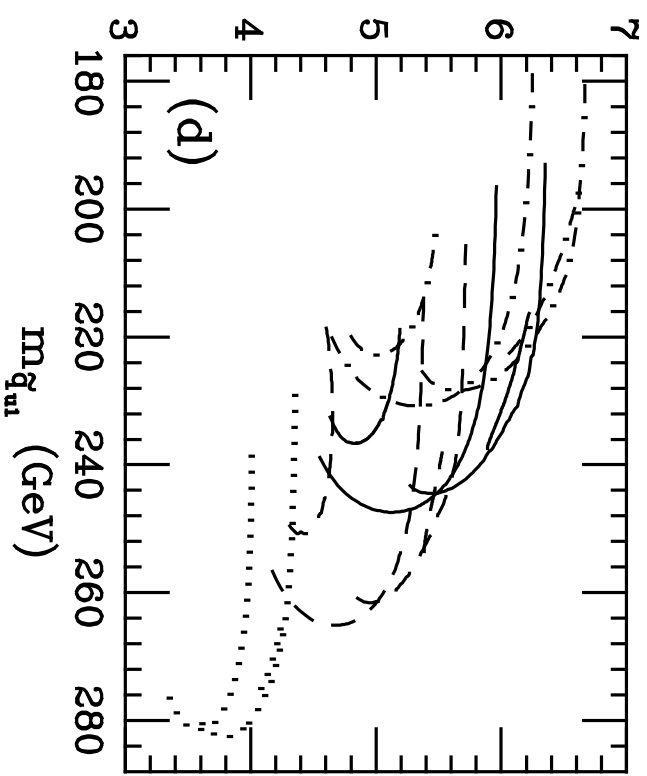
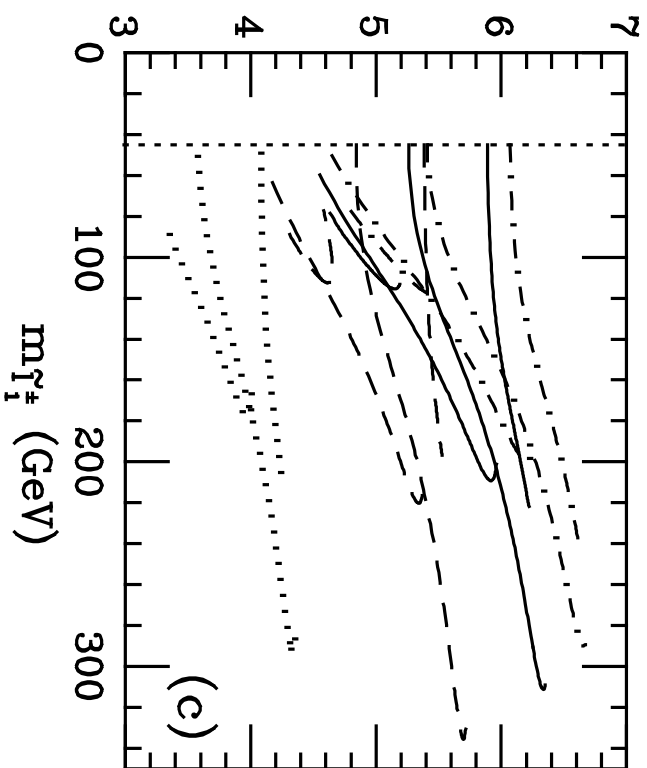
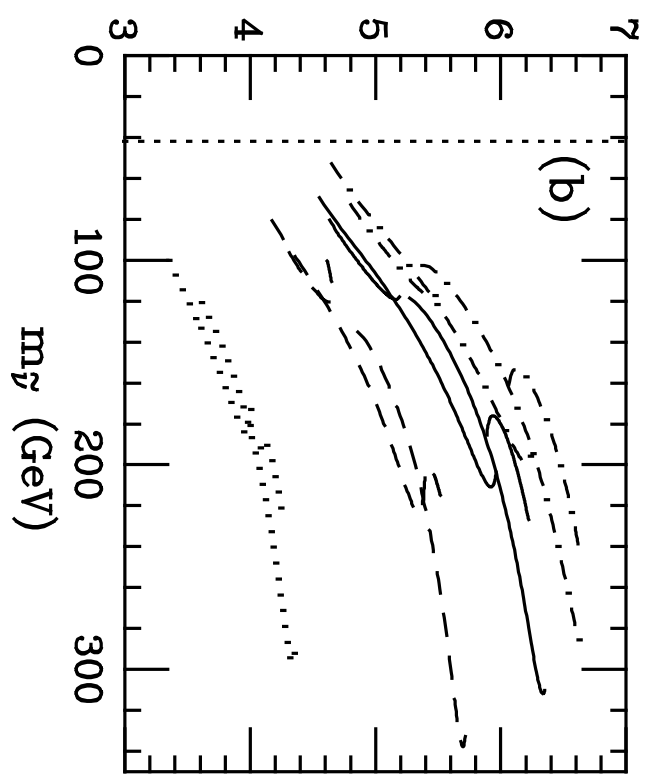
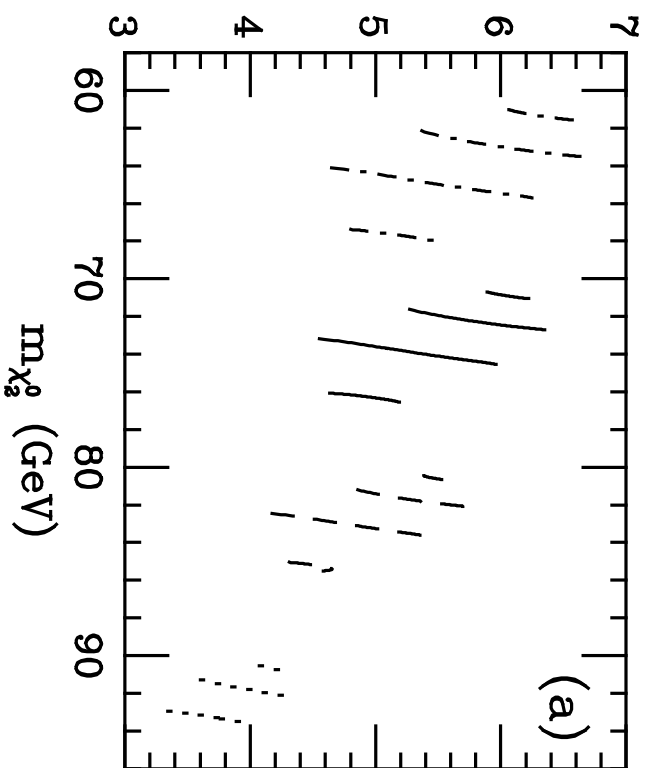


Fig. 3